

# Broad Beam and Ion Microprobe Studies of Single-Event Upsets in High Speed 0.18 $\mu$ m Silicon Germanium Heterojunction Bipolar Transistors and Circuits

Robert A. Reed<sup>1</sup>, Paul W. Marshall<sup>2</sup>, Jim Pickel<sup>3</sup>, Martin A. Carts<sup>4</sup>, Tim Irwin<sup>5</sup>, Guofu Niu<sup>6</sup>, John Cressler<sup>7</sup>, Ramkumar Krithivasan<sup>6</sup>, Karl Fritz<sup>8</sup>, Pam Riggs<sup>8</sup>, Jason Prairie<sup>8</sup>, Barbara Randall<sup>8</sup>, Barry Gilbert<sup>8</sup>, Gyorge Vizkelethy<sup>9</sup>, Paul Dodd<sup>9</sup>, Kenneth A. LaBel<sup>1</sup>

1. NASA/GSFC, Code 561.4, Greenbelt, MD 20771
2. Consultant, Brookneal, VA 24528
3. PR&T, Inc., Fallbrook, CA 92028
4. Raytheon ITSS, Greenbelt, MD, 20771
5. Jackson & Tull Chartered Engineers, Washington, D. C. 20018
6. Auburn University, Auburn Al , 36894
7. Georgia Institute of Technology, Atlanta, GA 30332
8. Mayo Foundation, Rochester, MN 55905
9. Sandia National Labs, Albuquerque, NM 87185

**Abstract**—Combining broad-beam circuit level SEU response with ion microprobe tests on single silicon germanium heterojunction bipolar transistors allows for a better understanding of the charge collection mechanisms responsible for SEU response of HBT technology.

## Corresponding and Presenting Author:

Robert A. Reed, NASA/GSFC, Code 561.4, Greenbelt, MD 20771, phone: 301-286-2153, email: [Robert.A.Reed@nasa.gov](mailto:Robert.A.Reed@nasa.gov)

## Contributing Authors:

Paul W. Marshall, Consultant, 7655 Hat Creek Road, Brookneal, VA 24528, phone: 434-376-3402, email: [PWMarshall@aol.com](mailto:PWMarshall@aol.com)

J.C.Pickel, PR&T, Inc., 1997 Katie Ct., Fallbrook, CA 92028, phone: 460-451-5526, fax: 309-273-8483, e-mail: [jim@pickel.net](mailto:jim@pickel.net)

Martin A. Carts, Raytheon ITSS, c/o NASA/GSFC, Code 561.4, Greenbelt, MD 20771, phone: 301-286-2600, email: [mcarts@pop500.gsfc.nasa.gov](mailto:mcarts@pop500.gsfc.nasa.gov)

Tim Irwin, QSS, c/o NASA/GSFC, Code 561.4, Greenbelt, MD 20771, phone: 301-286-2014, email: [tirwin@pop500.gsfc.nasa.gov](mailto:tirwin@pop500.gsfc.nasa.gov)

Guofu Niu and Ramkumar Krithivasan Auburn University, 200Broun Hall, ECE Dept., Auburn Al , 36894, phone 334-844-1856

John Cressler, Georgia Institute of Technology, School of ECE, 791 Atlantic Dr., Atlanta, GA 30332

Karl Fritz, Pam Riggs, Jason Priere, Barbara Randall, and Barry Gilbert, Mayo Foundation, 200 1st Street SW Rochester, MN 55905, phone:507-538-5481, email: [randall.barbara@mayo.edu](mailto:randall.barbara@mayo.edu)

Gyorge Vizkelethy, Sandia National Labs, P.O. Box 5800, MS1056, Albuquerque, NM 87185, phone: 505-284-3120,

Paul Dodd, , Sandia National Labs, P.O. Box 5800, MS1083, Albuquerque, NM 87185, phone: 505-844-1447

Kenneth A. LaBel, NASA/GSFC, Code 561.4, Greenbelt, MD 20771 (USA), phone: 301-286-9936, email: [Kenneth.A.Label@nasa.gov](mailto:Kenneth.A.Label@nasa.gov)

**Session Preference:** I am undecided SEE: basic mechanisms or SEE: Devices and ICs (?Any suggestions?)

**Presentation Preference:** Oral

## I. Introduction

SiGe based technology is widely recognized for its tremendous potential to impact the high speed microelectronic industry, and therefore the space industry, by monolithic incorporation of low power complementary logic with extremely high speed SiGe Heterojunction Bipolar Transistor (HBT) logic. A variety of studies have examined the ionizing dose, displacement damage and single event characteristics, and are reported in [1 and references therein]. Accessibility to SiGe through an increasing number of manufacturers adds to the importance of understanding its intrinsic radiation characteristics, and in particular the single event effect (SEE) characteristics of the high bandwidth HBT based circuits. IBM is now manufacturing in its 3rd generation of their commercial SiGe processes, and access is currently available to the first two generations (known as 5HP and 6HP) through the MOSIS [2] shared mask services with anticipated future release of the latest (7HP) process. The 5HP process is described in [1 and references therein] and is characterized by a emitter spacing of 0.5  $\mu\text{m}$  and a cutoff frequency  $f_T$  of 50 GHz, whereas the fully scaled 7HP HBT employs a 0.18  $\mu\text{m}$  emitter and has an  $f_T$  of 120 GHz.

Previous investigations have examined the SEE response of 5HP HBT circuits through both circuit testing [3] and modeling [4-5]. Charge collection modeling studies in the 5HP process have also been conducted [6], but to date no measurements have been reported of charge collection in any SiGe HBT structures. Nor have circuit models for charge collection been developed in any version other than the 5HP HBT structure. Our investigation reports the first indications of both charge collection and circuit response in IBM's 7HP-based SiGe process. We compare broad beam heavy ion SEU test results in a fully function Pseudo-Random Number (PRN) sequence generator up to frequencies of 12 Gbps versus effective LET, and also report proton test results in the same circuit. In addition, we examine the charge collection characteristics of individual 7HP HBT structures and map out the spatial sensitivities using the Sandia Focused Heavy Ion Microprobe Facility's Ion Beam Induced Charge Collection (IBICC) technique [7]. Combining the two data sets offers insights into the charge collection mechanisms responsible for circuit level response and provides the first insights into the SEE characteristics of this latest version of IBM's commercial SiGe process.

## II. Broad Beam Testing of the 7HP PRN

### II.A Device Description and Test Setup

The device is a  $2^7-1$  Pseudo-Random Number (PRN) sequence generator fabricated in IBM 0.18  $\mu\text{m}$  (7HP) SiGe process. It was designed by the Special Purposes Processor Group (SPPG) at Mayo Foundation and fabricated by IBM under a DARPA contract. It consists of 7 flip-flops in series that generate a known sequence of 127 bits known as 7 bit Pseudo-Random Number (PRN-7) sequence. The device is capable of producing digital data streams at greater than 12 GHz.

The test setup will be completely described in the final paper. We summarize here: The heart of the test system is the Anritsu MP1764A, a 12.5 Gbps Bit Error Rate Tester (BERT). The BERT was programmed to interrogate the incoming bit stream for errors. When an error occurred the BERT passed an error flag to the control PC, which was used as an error counter and to reset the PRN. Errors were tallied for each run and a reset cross-sections to be computed.

### II.B Experimental Reset Error Results

Heavy ion testing was carried out at Texas A&M University Cyclotron Facility. These data represent the first measure of the SEU sensitivity of the any device fabricated in IBM 0.18  $\mu\text{m}$  SiGe HBT.

In order to achieve the desired ion LETs with sufficient range into silicon we used a combination of neon at 40 MeV/amu, argon at 40 and 15 MeV/amu and Krypton at 15 MeV/amu. Testing was carried out using at least five angles of incidence, 0, 30, 45, 60, 72 degrees.

Figure 1 is a log-log plot of the cross-section for PRN resets when exposed to heavy ion's with various effective LETs. As is typically done for heavy ion exposures, the normal incidence fluence and LET have been corrected

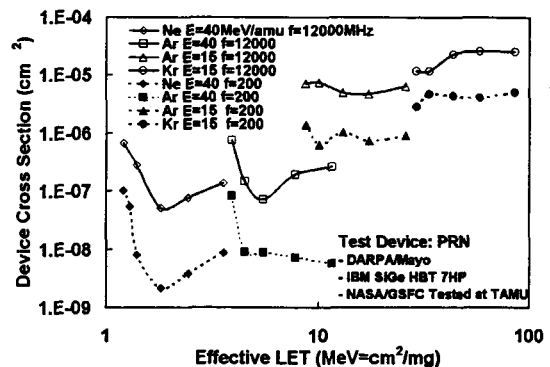


Figure 1. Cross-section results on PRN

using the  $1/\cos(\theta)$  factor to determine the “effective” cross-section and the “effective” LET, respectively.

The data connected by solid lines are for a 12 GHz serial data stream, those connected by the dashed lines are for 0.2 GHz. Each symbol type represents a different normal incident ion LET. Note that the data in Figure 1 show that the “effective” cross-section decreases with increasing “effective” LET by nearly two orders of magnitude for low LET values (an effect that is consistent with the SEU data on the IBM 5HP technology [3]). Also note that this is apparent at both data rates, this data rate dependence is consistent with results from the IBM 5HP technology reported in [3] and other high speed circuits [references contained in 3]. (Data collected at other frequencies will be presented in the final paper, these data follow the trends in Fig 1). Finally note that the data show that the threshold LET for this device is less than  $1.8 \text{ MeV}\cdot\text{cm}^2/\text{mg}$ . This very low threshold is also consistent with the data on the IBM 5HP [3].

(We will present proton-induced SEU data in the final manuscript. Here we simply state that proton-induced errors were observed and are consistent with the heavy ion results.)

### III. Microbeam Testing of 7HP HBT

#### III.A Device and Test Setup

Sandia National Laboratory’s focused heavy ion microprobe facility [7] was used to interrogate the amount of charge collected by each terminal of a single SiGe 7HP HBT transistor.

The die had a single  $0.18 \times 19.2 \mu\text{m}^2$  transistors bonded out. Transistor cross-sectioning and SEM images (SEMs) were performed prior to microbeam testing. The right image of Figure 2 shows the SEMs of a 7HP Transistor. The left portion of the figure shows a cartoon of the physical layout of the transistor and identifies the location of the base, emitter and collector contacts among other things. A complete description will be given in the final manuscript, for the summary we will highlight the key parameters.

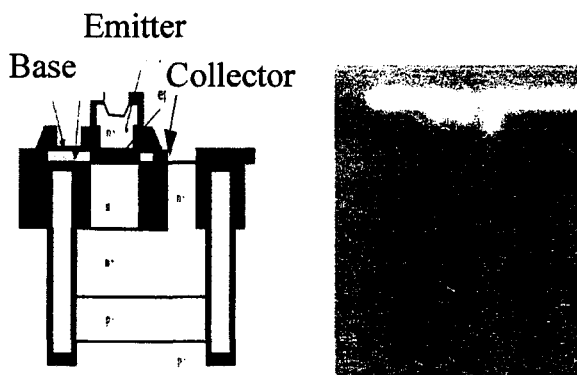


Figure 2 Left: cartoon of SiGe HBT layout.  
Right: SEM of 7HP HBT

The transistor is almost entirely silicon, the germanium is contained in the small base region. The transistor is totally contained inside two insulating trenches—a shallow trench and a deep trench—that completely outline the transistor area. The collector contact is electrically connected to the large volume confined by the deep trench. The trench is  $\sim 3.0 \times 20.5 \mu\text{m}^2$ . The bottom of the deep n+ layer is approximately  $5 \mu\text{m}$  for the top of the silicon and the deep trench reaches  $\sim 7 \mu\text{m}$  into the silicon.

The die was exposed to a chemical vapor etch process to remove any polyimide that was on top of the die—this etch was required so that ions could penetrate  $>15 \mu\text{m}$  into the silicon. After etching there was approximately  $7.6 \mu\text{m}$  dead layer that consisted of several alternating metal/insulator layers plus passivation layers.

A four probe IBICC measurement [7] was used to simultaneously measure the charge presented on the Collector (C), Emitter (E), Base (B), and substrate (Sx) terminal due to a series of ion strikes occurring in and around the Transistor area. The beam was stepped across an area of the die that contained the transistor. The data cube is built up by several scans of the large area and consists of the location of the ion spot (X and Y coordinates) and the charge collected by each probe.

An Agilent 4156 parametric analyzer was used to measure forward and reverse Gummel plots before and after each run. Pre- and post-irradiation plots showed no degradation of transistor performance.

#### III.B Microbeam Results on $0.18 \mu\text{m}$ HBT

The IBICC measurements were made using 36 MeV oxygen ions. The range of these ions in silicon is  $24.5 \mu\text{m}$ , giving greater than  $17 \mu\text{m}$  of penetration in the active layer of the device. For all tests the ion beam spot size was near  $2 \mu\text{m}^2$ . The total area exposed during one sweep (or scan) was near  $1600 \mu\text{m}^2$ . The step size was near  $0.1 \mu\text{m}$ . The two test conditions were: 1) E,B,C,Sx grounded, 2) E,B,C grounded, Sx set to  $-5.2\text{V}$

Figure 3 shows a 3D smoothed fit to the charge collection results obtained on the HBT collector with the substrate biased at  $-5.2\text{V}$ . The charge, fC, collected is plotted as a function of X and Y position (the full manuscript will show the plots for the emitter, base and substrate for each bias condition, herey we focus on the key results).

At first glance there appears to be a well-defined charge collection volume that is approximately the same size as the deep trench isolation. Any ion event occurring in the deep trench causes nearly the same amount of charge to be collected at the collector contact. The collector is the SEU sensitive node for the standard master-slave flip-flop configuration [5]—used in the PRN. The entire trench volume defines a portion of the SEU sensitive volume—but not the entire sensitive volume!

Careful inspection of these data reveal that a small, but measurable amount of charge is collected when the ion event is outside the trench—note the light gray (small charge collection) circular area surrounding the dark (large charge collection) rectangular shaped area. These events can cause a circuit to upset if there is sufficient charge collection, this will increase the size of the sensitive volume. We will discuss this in further detail in the next section.

## IV Discussion and Analysis

### IV.A. Cross-Section Angular Dependence

The data in Figure 1 show that, for low LETs, there is an initial large drop in the cross-section followed by a slight increase as the beam angle is rotated from 0 to 72 degrees. These data cannot be fitted using a simple Rectangular Parallel-Piped (RPP) model for the sensitive volume. (This was noted in [3] with regards to the IBM 5HP HBT technology, implying that this is a potential concern for all HBT technologies.)

One explanation for obscure data has been to argue that there is a different sensitivity do to edge effects for very thick sensitive volumes. The Heavy Ion Cross-section for single event Upset (HIC-UP) model [8] has been used to account for edge effects in the RPP model. We have reviewed this model and determined that, for the sensitive volume dimensions consistent with the IBM HBT technology, the largest decrease in the cross-section would be near a factor of 5—much less than the factor of 90 observed from the experimental cross-section data. (We will give the details of this calculation in the final paper).

### IV.B. Implication of Charge Diffusion

A limit on the critical charge for the PRN can be estimated by assuming a charge collection depth between 7 and 12  $\mu\text{m}$  (this is consistent with the deep trench and with device simulations on the 0.50  $\mu\text{m}$  technology [9]). Using this and the fact that the threshold LET is  $< 1.8 \text{ MeV}\cdot\text{cm}^2/\text{mg}$  an upper limit for the critical charge for this device is less than 150 fC, and could be as low as 50 to 100 fC.

The data in Figure 4 give a 1  $\mu\text{m}$  wide slice of the data plotted for collector events in Figure 3. The data is for a 1  $\mu\text{m}$  wide slice center on  $Y=19.5 \mu\text{m}$ , all data is projected onto the X-axis for this 2D plot of the charge collected as a function of X position. The smaller charge collection events occurring outside trench have values  $> 75$  fC for distances as far as 5  $\mu\text{m}$  away from the deep trench. There is significant amount of charge collected by the collector contact from carriers that are generated in the substrate region beyond the trench—enough to cause an upset in several circuit types, the PRN described in this paper is one example.

A certain portion of the sensitive volume that is defined by the silicon confined inside the deep trench. There is also a portion of the sensitive volume that is solely due to charge collected by diffusion of charge in the substrate region beyond the trench. This significantly complicates the structure of the sensitive

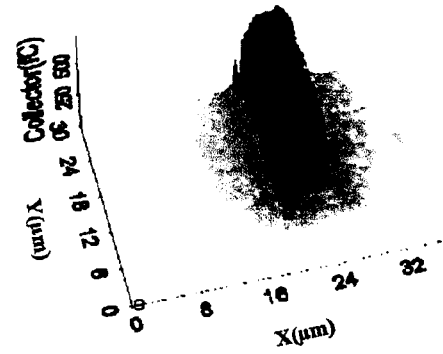


Figure 3. 3D IBICC plot of charge collected by collector of 7HP HBT

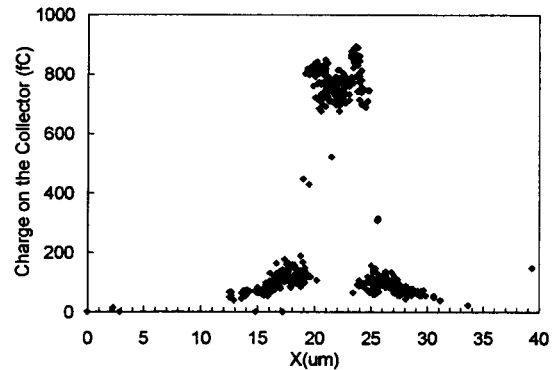


Figure 4. 1  $\mu\text{m}$  wide cross-section of the 3D data plotted in figure 3 centered on 19.5  $\mu\text{m}$ .

volume, i.e. it is no longer an RPP. The exact details of the dimensions of the portion of the sensitive volume that is due to diffusion charge outside the trench will depend on the ion angle of incidence, the critical charge of the device, the ion's LET, and the diffusion length of the carriers in the substrate. This complex structure is one plausible explanation for the data trends observed in Figure 1.

#### IV.C. Modeling

Charge collection in the test structure was modeled using a Monte Carlo model in a modified version of the REACT code [10]. The model tracks carriers generated along the ion path until they are either collected in a high-field depletion region, recombine at a recombination surface, or exceed the carrier lifetime. The carriers are transported by diffusion and drift, including spatially variant electric fields, and those that reach a chosen surface are either counted or recombined. The structure that was modeled is shown in Fig. IV.2. The interior region represents a  $3\ \mu\text{m} \times 21\ \mu\text{m}$  charge collection structure that is  $5\ \mu\text{m}$  thick. Any charge that is generated in this volume or generated outside the volume and then diffuses to the surface of the volume is assumed to be collected. Surrounding the charge collection region is a  $1\ \mu\text{m}$  wide oxide isolation trench that is  $7\ \mu\text{m}$  deep. Any charge generated in this volume or diffusing to the surface of this volume is recombined. An example analysis is shown for three cases of a 22.5 MeV oxygen ion. For the example, the regions outside the collection region and the isolation trench are assumed to have zero electric field and charge spreads from the ion track only by diffusion. A diffusion length of  $27\ \mu\text{m}$ , corresponding to a mobility of  $1000\ \text{cm}^2/\text{V}\cdot\text{s}$  and a lifetime of 290 ns, was assumed. In case 1, the ion penetrated the collection volume at normal incidence, with the impact point indicated by "X". Charge is collected by drift along the  $5\ \mu\text{m}$  path through the high-field region and then by diffusion from the zero-field region below. In case 2, the ion penetrated at normal incidence with an impact point outside but near the isolation trench, also indicated by "X". All of the charge is generated outside the structure. The charge that diffuses over the "wall" presented by the isolation trench is collected if the carrier reaches the high field surface  $2\ \mu\text{m}$  below the "wall". In case 3, the ion penetrated at the same point as case 2 but with an angle at 60 degrees from normal and directed toward the charge collection volume. All charge generated along the slant path through the high-field region is collected and additional charge is collected by diffusion from the zero-field regions. Table 1 shows the charge collected by drift in the high-field region and by diffusion for zero-field regions.

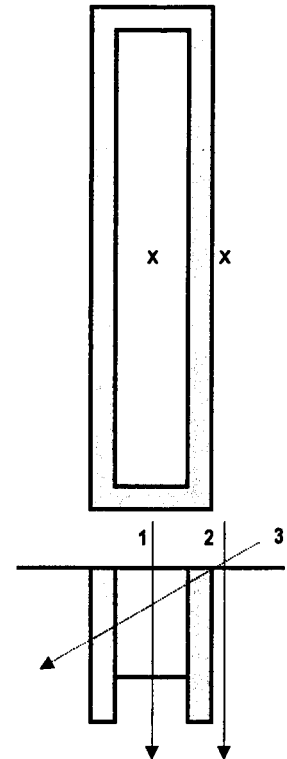


Figure 1. Top view and a cross-section view of trench are shown.

For the paper, the model will be applied to specific experimental cases and compared to the experimental results.

#### IV Conclusions

We present the first broadbeam SEU and microbeam IBICC results on IBM 7HP HBT. Combining the two data sets demonstrated insights into the charge collection mechanisms responsible for circuit level response. Detail knowledge of the charge collection due to diffusion is required to completely describe the sensitive volume for these HBT.

#### IV References

[1] John D. Cressler and Goufu Niu, Silicon-Germanium HBTs, Artech House, 2002  
 [2] <http://www.mosis.org/Products/menu-products.html>  
 [3] P.W. Marshall, et. al IEEE TNS, Vol. 47, No. 6, December 2000, pp. 2669-2674.  
 [4] G. Niu, et. Al, IEEE TNS, Vol. 48, No. 6, December 2001, pp. 1849-1858  
 [5] G. Niu, IEEE TNS, Vol. 49, No. 6, 2002, pp. 3107-3114

Table 1. Results for example charge collection modeling of a structure similar to the test devices.

Case	1	2	3
Location	12,3	12,6	12,6
$Q_{\text{depletion}}$	1.95e6	0	1.35e6
$Q_{\text{diffusion}}$	7.97e4	2.23e4	3.68e4

[6] J. D. Cressler, IEEE TNS, Vol. 47, No. 6, December 2000, pp. 2682-2689.  
 [7] G. Vizkelethy, 2002 NSREC Radiation Data Workshop Record  
 [8] L. Connell, et. Al, IEEE TNS, Vol. 43, No. 6, December 1996, pp. 2682-2689  
 [9] Private communication with Guofu Niu  
 [10]. J.C.Pickel, et. al, IEEE TNS, Vol. 49, No. 6, P.2822, December 2002